

CFD-DEM simulations and experimental validation of clustering phenomena and riser hydrodynamics

A.E. Carlos Varas, E.A.J.F. Peters*, J.A.M. Kuipers

Department of Chemical Engineering and Chemistry, Multiphase Reactors Group, Eindhoven University of Technology, Eindhoven, The Netherlands

HIGHLIGHTS

- Full-field experimental validation of CFD-DEM of riser hydrodynamics is presented.
- Special attention is paid to the characterisation of particle clusters.
- Properties of particle cluster are predicted well by CFD-DEM.

ARTICLE INFO

Article history:

Received 15 May 2016

Received in revised form

18 July 2016

Accepted 18 August 2016

Keywords:

CFD-DEM

Riser

CFB

PIV

Experimental validation

Particle

Clusters

ABSTRACT

A combined numerical and experimental study of riser hydrodynamics is reported for the fast fluidisation regime. The experimental data sets are used for validation of the CFD-DEM simulations. Special attention is paid to the formation of heterogeneities in the particle distribution, i.e., the formation of clusters. Application of Particle Image Velocimetry (PIV) in combination with Digital Image Analysis (DIA), provides a complete data set for the particle flow in a pseudo-2D riser. A CFD-DEM model is employed to simulate the co-current gas-particle flow. Particle clusters are detected and characterised in our CFD-DEM simulation results and compared to experimental data. Core-annulus flow is well predicted by the model and other hydrodynamic parameters such as cluster frequency, internal solids volume fraction and aspect ratio were also in good agreement with experimental data.

© 2016 Elsevier Ltd. All rights reserved.

1. Introduction

Circulating fluidised beds are widely employed in industry for gas-solid contacting operations. These systems consist of a riser unit, where usually the main reaction takes place; and a downcomer that could be either employed as a reservoir or as a reactor in which a secondary process takes place. Riser hydrodynamics is characterised by the so-called core-annular flow, featuring a gas-solid cocurrent flow in the core of the reactor and a solids downflow close to the walls. Particle collisions promote the formation of particle clusters, which is especially important close to the walls of these systems. It is known that clusters generate a poor contacting between the gas and solids phase, leading to severe process efficiency losses. Thus, an accurate prediction of cluster-related properties is essential to attain an accurate prediction of riser reactor performance.

For this aim, riser hydrodynamics have been extensively investigated over the last decades. Mass and heat transfer phenomena sensitively depend on riser hydrodynamics. Gas and solids phase contact efficiency has been shown to significantly influence the performance of riser reactors (Guenther and Breault, 2007). Thus, an accurate representation of clustering properties is believed to be essential to accurately predict the overall conversion rates of chemical processes (Sundaresan, 2013). Clusters have been detected by means of optical probes in riser flows (Manyele et al., 2002; Soong et al., 1993; Sharma et al., 2000) using Soong et al. cluster criteria (Soong et al., 1993). Despite all studies reported in literature, clusters do not have a clear definition (Harris et al., 2002) and it has been suggested that cluster definition based on local flow fluctuations is not suitable to quantify clustering (Johnsson and Johnsson, 2001; Guenther and Breault, 2007; Carlos Varas et al., 2016b). Wavelet decomposition techniques seem to capture well the meso-scale signals due to the presence of clusters, enabling in-depth analysis of operating conditions (Chew et al., 2012). However, the detection of these structures is not straightforward and are mostly limited to local or sectional

* Corresponding author.

E-mail address: E.A.J.F.Peters@tue.nl (E.A.J.F. Peters).

Nomenclature*Roman symbols*

d_p	particle diameter, m
\mathbf{F}_c	particle collision force, N
$\langle G_s \rangle$	time-averaged axial solids mass flux, kg/(m ² •s)
I_p	moment of inertia, N•m
m	mass, kg
P	pressure, Pa
\mathbf{r}	position vector, m
\mathbf{s}_p	solids displacement vector, m
\mathbf{S}_p	momentum source term, N/m ³
\mathbf{T}_p	torque, N•m
\mathbf{u}	gas velocity vector, m/s
\mathbf{v}_p	particle velocity vector, m/s
V_p	particle volume, m ³
$\bar{\mathbf{v}}_p$	grid-averaged particle velocity vector, m/s

W	width of pseudo 2D domain, m
x/W	dimensionless riser width (-)

Greek symbols

Δt_{Gas}	gas phase time step, s
Δt_{DEM}	particle phase time step, s
β	interphase momentum transfer coefficient, kg/(m ³ •s)
ρ_g	gas density, kg/m ³
ρ_s	solids density, kg/m ³
μ	dynamic viscosity, kg/(m•s)
$\varphi_{cluster}$	cluster phase holdup, m ³ cluster/m ³ reactor
φ_s	solids volume fraction, m ³ solid/m ³ reactor
θ	granular temperature, m ² /s ²
$\boldsymbol{\tau}$	stress tensor, Pa
$\boldsymbol{\omega}_p$	particle rotational velocity, 1/s

measurements, without providing an overall quantification of clusters of the whole system.

A lot of numerical studies have been reported in order to predict the performance of fluidised systems. However, fully resolved simulations involve a very high computational cost, making necessary the employment of closures for particle-unresolved large scale simulations. Kinetic theory of granular flows (Lun et al., 1984) has enabled two fluid model (TFM) simulations of relatively large CFB's (Tsuo and Gidaspow, 1990; Panday et al., 2014; Cabezas-Gómez et al., 2008; Wang et al., 2008; Mathiesen et al., 2000). However, with affordable grid resolution particle clusters can typically not be resolved. This makes it necessary to use an effective description of these mesoscopic structures. An example of such a description is the energy minimisation methods (EMMS) (Li and Kwauk, 1994; Wang, et al., 2008; Lu et al., 2014; Shuai et al., 2012). Nowadays, energy minimisation models seem to be well accepted in the field to predict time-averaged solids content of riser systems; and clustering in riser flows. However, there are still some uncertainties about the accuracy of EMMS models to predict cluster-related properties, such as cluster size and porosity (Cheng et al., 2012). This is mainly due to assumptions that are implicit in EMMS models; some of these are that clusters have uniform density and equal to minimum fluidisation packing fraction (Naren et al., 2007); clusters are spherical, homogeneously dispersed structures that interact with a lean surrounding phase (Hartge et al., 2009); and no consideration is taken regarding particles rotation, which can be an additional cause of energy dissipation (Goldschmidt et al., 2004). TFM coupled to EMMS (Lu et al., 2008; Cheng et al., 2012) and stochastic Eulerian-Lagrangian models have been shown to predict well core-annular flow and some cluster parameters quantitatively at a limited number of axial positions and operating conditions (Shuyan et al., 2005; Wang et al., 2009a).

In CFD-DEM particle displacement and collisional forces are fully accounted for to capture the dynamic density feature of clusters that cannot be simulated with Euler-Euler models. In Euler-Lagrangian models, the particles motion is computed by means of Newton's second law; collisional forces and gas particle interaction are deterministically computed. These phenomena are inherent to cluster formation. Therefore CFD-DEM appears to be a suitable model to study cluster behaviour. Nevertheless, compared to TFM simulations, computational expenses are significantly higher, historically limiting the application of CFD-DEM to small scale systems. Nowadays, code parallelisation techniques can be very promising to make feasible future large scale simulations. Significant efforts are being made on the parallelization of CFD-

DEM codes (Jajcevic et al., 2013; Walther and Sbalzarini, 2009; Yang et al., 2015), simulations of granular flows of 117 million of particles are nowadays feasible (Tsuzuki and Aoki, 2016).

Previous research has been performed in the frame of Euler-Lagrangian simulations to predict clustering phenomena. It has been reported that particles do have an irregular motion and can be transferred from dilute to dense phase and vice versa (Ouyang and Li, 1999; Neri and Gidaspow, 2000). Tsuji et al. were among the pioneers in stating qualitative differences regarding cluster population when Euler-Lagrangian and Euler-Euler models were employed (Tsuji et al., 1998). Hoomans et al. (2000) revealed the strong influence of collisional parameters on clustering phenomena. Cluster formation has also been related to high slip velocities, revealing the influence of the non-linear drag force coefficient over clustering phenomena (Helland et al., 2007; Agrawal et al., 2001; Li and Kuipers, 2003). Clusters form due to inelastic collisions (Hoomans et al., 1996), whilst a higher gas-solid interaction leads to more homogeneous systems (Li and Kuipers, 2007). Comparison between Euler-Lagrangian computational models and experimental data of cluster properties have been performed (Capecelatro et al., 2014; Shuyan et al., 2005; Shuyan et al., 2009; Cabezas-Gomez et al., 2008) applying either Soong et al. (1993) or Sharma et al. (2000) criteria without attaining an insight regarding the influence of operating conditions on cluster frequency or size, which could vary slightly due to the imposed criteria to detect clusters. Little or no data have been found regarding validation of the aforementioned cluster properties over the whole flow field. Thus, we perform a full-field computational validation of riser hydrodynamics, including several cluster characterisation techniques.

According to experimental observations of Horio and Kuroki, (1994), clusters have a core-wake structure (Horio and Kuroki, 1994). This was also reported by other authors (Yang and Zhu, 2015; Yerushalmi and Cankurt, 1979). Soong et al. (1993) and Sharma et al. (2000) defined clusters as groups of particles, which internal solids holdup was above $\langle \varphi_s \rangle + n \cdot \sigma$ (where $\sigma = \sqrt{\langle (\varphi_s - \langle \varphi_s \rangle)^2 \rangle}$) and size was at least one order of magnitude above the particle diameter. However, previous authors have argued (Guenther and Breault, 2007; Johnsson and Johnsson, 2001; Carlos Varas et al., 2016b) that cluster definitions based on solids volume fluctuations could lead to erroneous identification of dense particulate structures due to the variability of the employed threshold for solids volume fraction. Brereton and Grace (1993)

defined the intermittency index (γ) to quantify the solids segregation under riser flow conditions. Brereton and Grace (1993) argued that the solids fluctuations under riser flow conditions are higher when clusters are more frequently encountered, while these would be lower in more homogeneous flows (e.g. continuous solid annulus or very dilute regions).

The objective of this work is to test the reliability of an Euler-Lagrangian model to predict clustering phenomena, by performing a thorough comparison between computational and experimental data of hydrodynamic and cluster related parameters. Slip velocity, shape, size, frequency or even the aspect ratio of clusters can significantly alter local mass transfer effects through clusters or even change the gas phase residence time distribution in the system. Therefore it is of high interest to evaluate the accuracy of computational models to predict these cluster properties. For this purpose, we employ a CFD-Discrete Element Model (DEM) to generate computational data of a pseudo-2D riser system and perform a cluster search to characterize the prevailing flow structures in the domain. In our previous work (Carlos Varas et al., 2016b), we reported full-field experimental results of a compact pseudo 2D riser reactor. These data consist of axial and radial profiles of solids mass flux and solids volume fraction at different axial locations and superficial velocities. Besides, an extensive cluster characterisation was performed. In this paper, the reliability of a CFD-DEM model is tested with full-field experimental measurements, including full-field measurements of cluster properties at several gas superficial velocities.

2. CFD-DEM

A CFD-DEM has been employed to carry out simulations of the flow in a pseudo-2D riser unit (Carlos Varas et al., 2016a). Navier-Stokes and continuity equations are solved to compute the flow patterns of the gas phase by means of a finite difference method:

$$\frac{\partial(\varepsilon \rho_g \mathbf{u})}{\partial t} + \nabla \cdot (\varepsilon \rho_g \mathbf{u}) = 0 \quad (1)$$

$$\frac{\partial(\varepsilon \rho_g \mathbf{u})}{\partial t} + \nabla \cdot (\varepsilon \rho_g \mathbf{u} \mathbf{u}) = -\varepsilon \nabla P - \nabla \cdot (\varepsilon \boldsymbol{\tau}) - \mathbf{S}_p + \varepsilon \rho_g \mathbf{g} \quad (2)$$

The gas and solids motion is coupled via a sink term that involves the computation of the interphase momentum transfer coefficient by means of the Beetstra drag correlation (Beetstra et al., 2007):

$$\mathbf{S}_p = \frac{1}{V_{\text{cell}}} \sum_{i=0}^{N_p} \frac{\beta V_p}{1 - \varepsilon} (\mathbf{u} - \mathbf{v}_p) D(\mathbf{r} - \mathbf{r}_p) \quad (3)$$

Two way coupling is performed by means of a regularised Dirac delta function $D(\mathbf{r} - \mathbf{r}_p)$, which maps the gas properties from neighbouring Cartesian nodes to the particle location to enable evaluation of the drag force. Moreover, changes in particle momentum are fed back from the particle position to the surrounding Eulerian nodes using the same regularised function (Deen et al., 2007).

The particle momentum is governed by the Newtonian equations of motion:

$$m_p \frac{d^2 \mathbf{r}_p}{dt^2} = -V_i \nabla P + \frac{\beta V_p}{1 - \varepsilon} (\mathbf{u} - \mathbf{v}_p) + m_p \mathbf{g} + \mathbf{F}_c \quad (4)$$

$$I_p \frac{d\boldsymbol{\omega}_p}{dt} = \mathbf{T}_p \quad (5)$$

The particle collision forces are deterministically computed, by means of a soft sphere model that was firstly proposed by Cundall and Strack (1979) and first employed in a gas fluidised system simulation by Tsuji et al. (1993). Gas turbulence was assumed to be insignificant compared to the velocity fluctuations due to gas-particle interaction, following other authors (Vreman et al., 2009; Helland et al., 2007). Thus, a sub grid turbulence model was not employed.

3. Simulation conditions

The dimensions of the simulation domain that correspond to the experimental pseudo-2D riser are $1.57 \times 0.07 \times 0.006$ m. In the experimental riser the outlet of the system is connected to a cyclone, where the gas-solid separation takes place. 0.8 mm glass beads were fed at an axial position of 7 cm above the gas distributor of the riser. The particles were fed from a storage vessel via a dosage slit with a small opening at the bottom-left side of the experimental unit. To facilitate smooth solids feeding to the riser, the particles were fluidised in the storage vessel at velocities close to u_{mf} (around 0.52 m/s). In experiments, the solids mass flux entering into the riser was determined by measuring the total height loss of the solids inventory in the downcomer in a time period of around 5 s. The solids mass flux at solids carryover conditions was of 32.0 ± 1.8 kg/m²s. However, when the solids entry was occasionally covered by particles, continuous solids feeding was not possible. In the same manner, this effect was implemented in the simulations. The particles were placed into random positions of the bottom X-Y plane, which area was equal to 0.07×0.006 m. An iterative procedure was placing particles into random positions of this plane. When a maximum of iterations (100) was reached without successfully finding a spot for a new particle, this one was not inserted. Thus, there could be occasionally lower solids mass fluxes than 32 kg/m²s due to the aforementioned entry blocking effects.

A curved wall of particles was placed at the top of the simulation domain to account for the influence of the lateral outlet that is present in the experimental setup. At the top, front, back and right walls, no-slip boundary conditions were applied. A prescribed inflow velocity u_0 was applied to the bottom X-Y plane of the domain. The left side wall ($x=0$) was subdivided into two regions: for the top-left outflow region of 0.07 m the pressure P_0 is described, and below this region a no-slip boundary conditions was set as Fig. 1b illustrates.

The top curved wall consisted of non-moving particles to mimic a lateral outlet present in the experiments. Gas and solid phases were leaving the domain at the top-left side outlet to simulate a system that closely resembled the experimental unit.

Collision parameters were those reported by Hoomans et al. (1996). The normal and the tangential restitution coefficient between the particles (glass beads) were 0.96 and 0.33, respectively. The restitution coefficient for the particle/stainless steel walls was set to 0.86 (including the solid particulate top-wall). The grid cell size is chosen to be about 3 particle diameters. In previous studies it has been shown that with computational cells of 2-4 particle diameters the hydrodynamics of heterogeneous (bubbling) gas-solid flows was captured well (Wang et al., 2009b). Additional simulation parameters are specified in Table 1.

The total simulation time was 20 s. In the post-processing the first 10 s were discarded to exclude start-up effects. Beyond that simulation time, pseudo steady state was attained.

Simulation data were collected each 0.005 s. Post-processing of simulation porosity data was performed to perform the cluster search over all the output files. These files were treated as 2D data fields to mimic the detection method performed in experiments (see Fig. 2b).

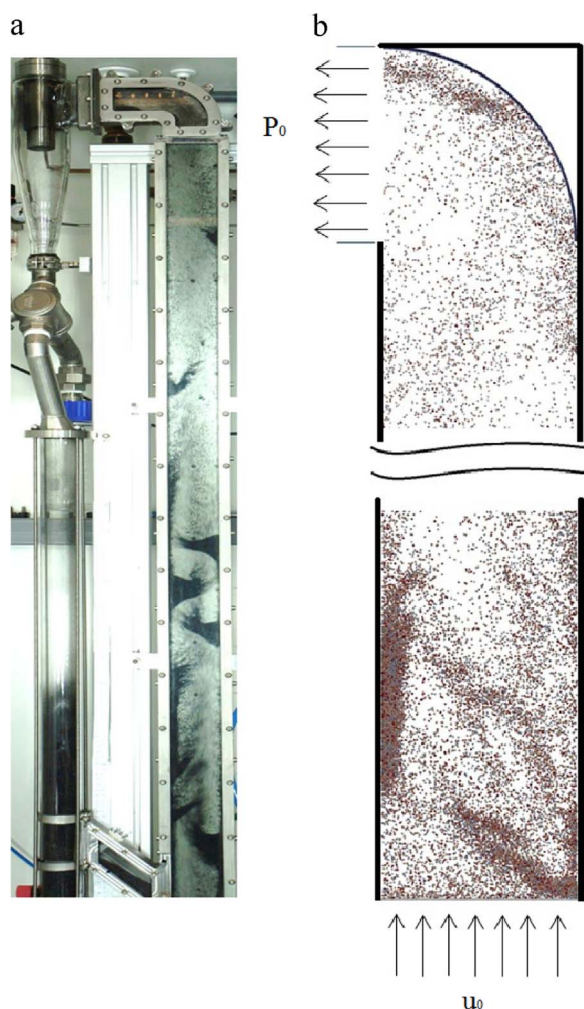


Fig. 1. a) Snapshot of experimental setup. b) pseudo-2D riser system in CFD-DEM model.

Table 1
Simulation parameters.

NX	28	d_p (mm)	0.85 ± 0.05
NY	5	ρ_s (kg/m ³)	2500
NZ	628	μ_g (kg/m·s)	$1.8 \cdot 10^{-5}$
X (m)	0.07	T (K)	298
Y (m)	0.006	e_{p-p}	0.96
Z (m)	1.57	e_t	0.33
Δt_{Gas} (s)	$5.0 \cdot 10^{-5}$	e_{p-w}	0.86
Δt_{DEM} (s)	$5.0 \cdot 10^{-6}$	μ_{fr}	0.15
Gs (kg/m ² s)	32.0	k_n (N/m)	1600
U (m/s)	5.55–6.74	P	1 atm

3.1. Cluster detection

A fast fluidised bed is characterised by a dense bottom zone and a dilute freeboard region at the top. There is also a solids holdup gradient in the non-stream wise direction with higher solids holdup close to the walls. As expected, solids fluctuations also change along the riser domain (Breerton and Grace, 1993; Johnsson and Johnsson, 2001; Carlos Varas et al., 2016b). Thus, constant solids holdup thresholds were employed along the entire domain of the pseudo-2D riser. In this way, it was ensured a uniform definition of cluster and that the quantified cluster-related properties were not only influenced by a changing definition along the axial and cross-sectional directions of the riser.

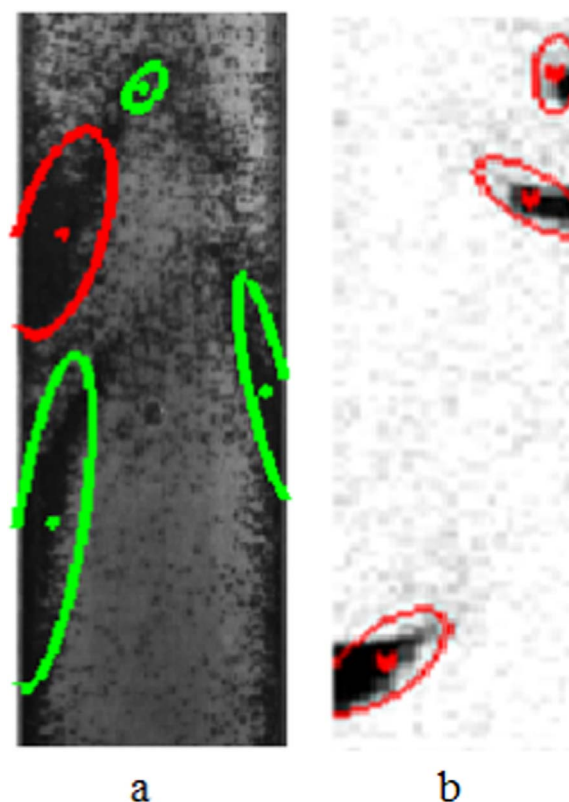


Fig. 2. The detected clusters. a) Experimental image b) Solids fraction field of CFD-DEM simulation.

Both in experiments and simulations clusters are defined as connected regions with local solids fractions larger than 0.2 everywhere that have a minimum (projected) area of 60 mm² and a dense core with at least one grid with $\varphi_s > 0.4$. To not attain too much noise in our measurements, only dense groups of particles that were one order of magnitude above the particle diameter in size were identified as clusters. The area of 60 mm² corresponds to an equivalent circle diameter of 8 mm. The detection of clusters was performed by post-processing experimental recordings and simulation data by means of a Matlab[®] script. In Fig. 2, clusters can be observed in both experiments and simulations. Green ellipses correspond to clusters moving upwards, while red ones move downwards. It is noted that dense clusters are formed close to the wall and tend to fall down, while big dilute strands of particles tend to move upwards.

4. Results and discussion

A computational study of the system described in previous sections was performed. Several superficial velocities were considered ($U=5.55, 5.95, 6.35$ and 6.74 m/s) at a solids mass flux of 32 kg/m²s.

4.1. Solids volume fraction

4.1.1. Axial profiles

Axial profiles of the solids volume fraction computed by means of the CFD-DEM simulation are compared to experimental results previously reported (Carlos Varas et al., 2016b). A key feature is that the comparison can be performed over the entire length of the riser, as a result of the full field nature of our experimental technique. In Fig. 3, it can be seen that computational and experimental results are in close agreement. At the lowest superficial velocity case ($U=5.55$ m/s), simulations describe a slightly denser

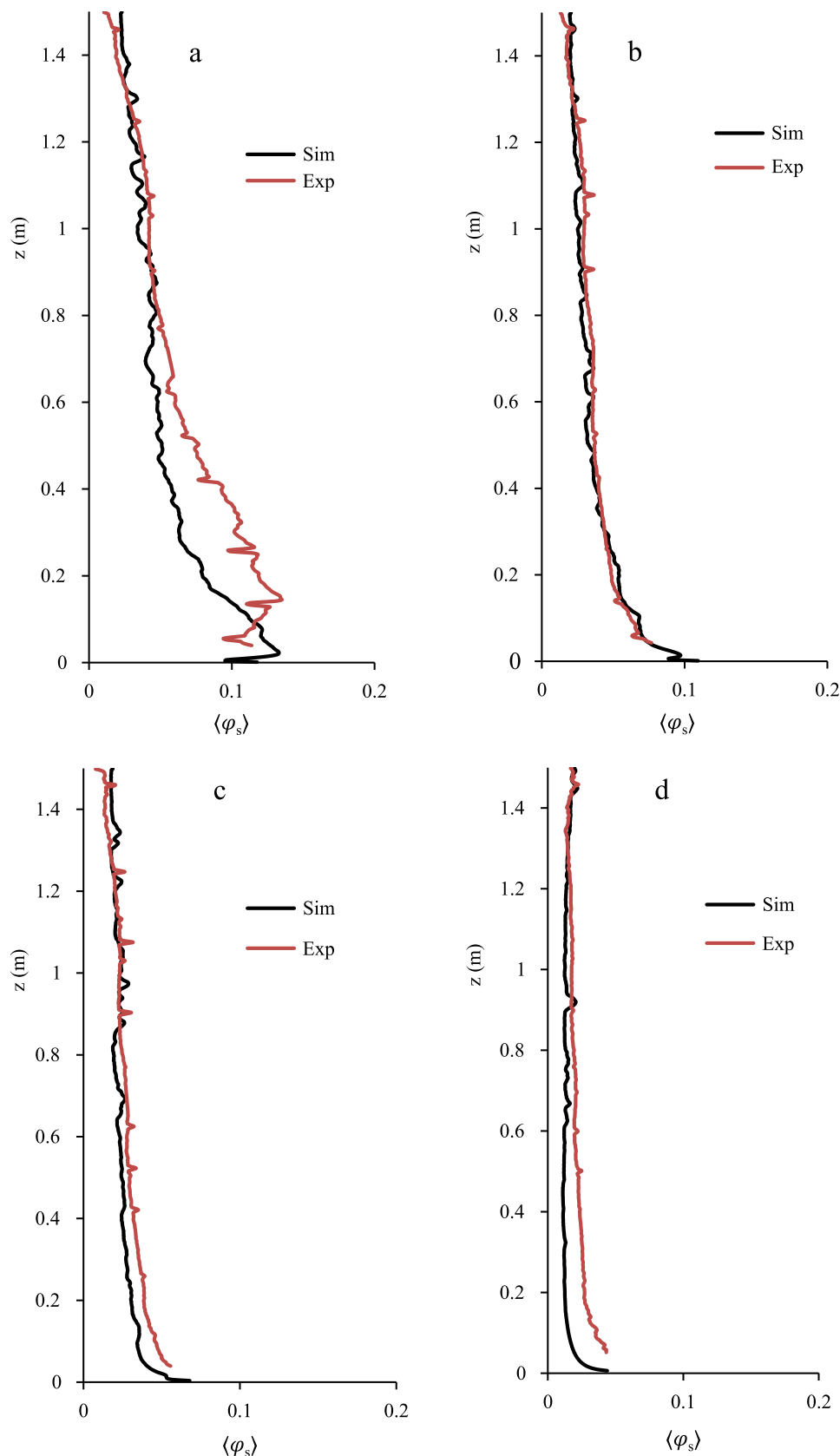


Fig. 3. Axial profiles of the time-averaged solids holdup. a) $U=5.55$ m/s. b) $U=5.95$ m/s. c) $U=6.35$ m/s d) $U=6.74$ m/s.

region at the bottom of the reactor, while the top region is more dilute than in experiments. At the highest superficial velocity case ($U=6.74$ m/s), it is noted that the model predicts a slightly more dilute system in comparison to the experiments.

4.1.2. Cross-sectional profiles

As part of a complete and a thorough validation of our model, cross-sectional profiles of the solids volume fraction are also compared at different superficial velocities and axial positions ($z=0.8, 1.1$ and

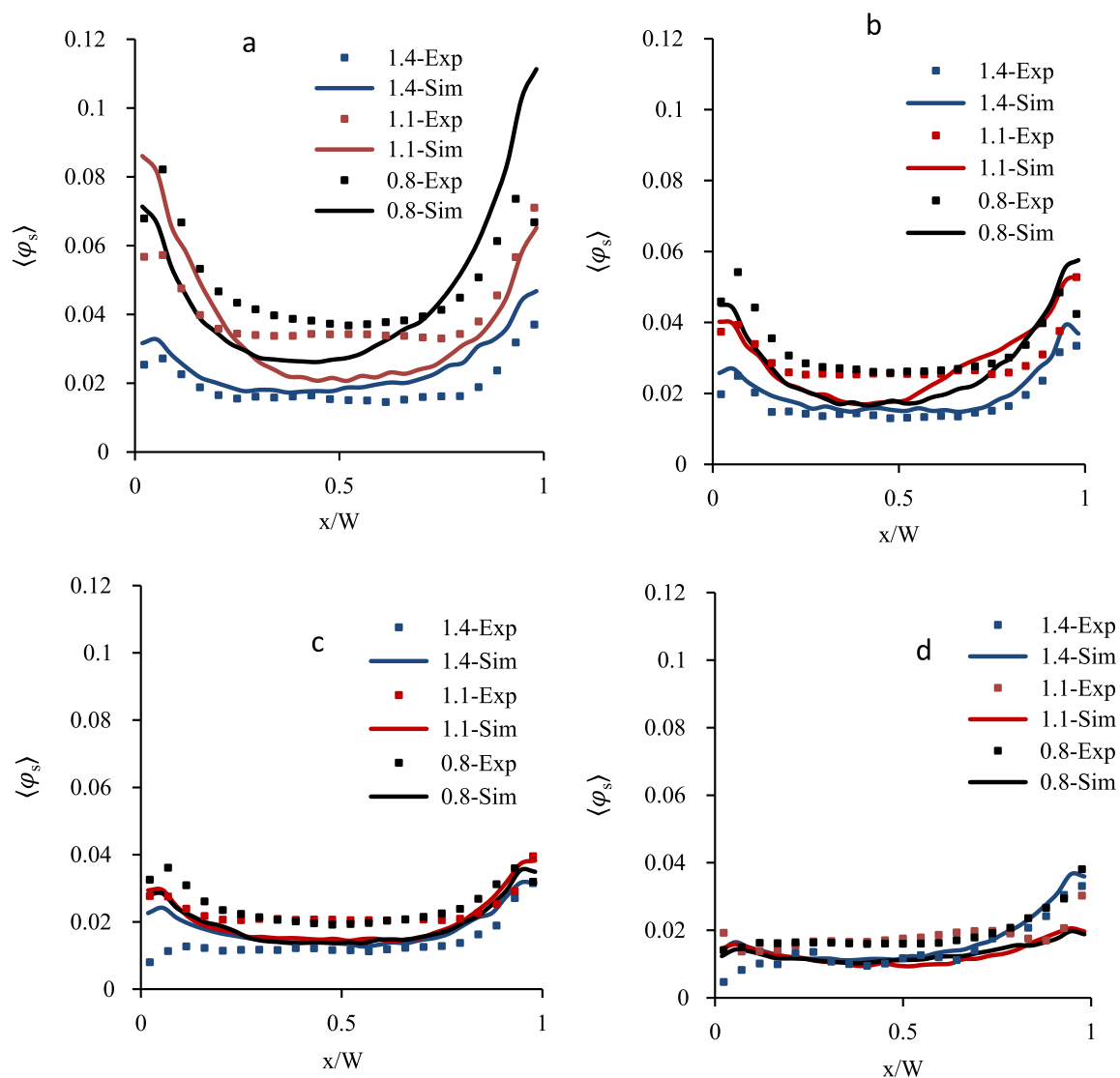


Fig. 4. Cross sectional profiles of solids volume fraction. a) $U=5.55$ m/s. b) $U=5.95$ m/s. c) $U=6.35$ m/s. d) $U=6.74$ m/s.

1.4 m). As expected, axial location and gas superficial velocity have a strong effect on the solids concentration profiles. At low superficial velocities, a pronounced solids holdup profile is captured between $z=0.8$ m and top sections ($z=1.4$) of the riser. Higher superficial velocities lead to more homogeneous systems with flatter profiles of the solids volume fraction.

As can be seen in Fig. 4, experimental and computational results are quite close to each other. A core-annulus shape is clearly visible in both experiments and simulations, while a clear asymmetry is observed at the highest superficial velocity case ($U = 6.74$ m/s). At such high velocities, the collisional frequency between the particles against the top curved wall increases, and generates a solids downflow at the right side wall ($x/W=1$).

4.2. Solids mass flux

Cross-sectional profiles of the solids mass flux are also illustrated in Fig. 5. As can be noticed, more significant differences can be perceived in these plots. Although, in terms of magnitude, experimental and computational profiles are close (especially at the riser core), qualitative differences are found close to the walls. These differences become more pronounced at high superficial velocities, where simulations describe flatter and less asymmetric

profiles than in experiments. So we can say that collisions with the top wall generate a stronger solids downflow in simulations than in experiments at high gas superficial velocities.

Solids volume fraction measurements were obtained by means of a DIA technique which requires a $2^{\text{D}}-3^{\text{D}}$ correlation. The relation between the measured 2D intensity and the wanted (3D) solids volume fraction is very steep beyond φ_s values of 0.3. This feature can lead to overestimation of solids volume fraction measurements when dense particle structures are encountered (Carlos Varas et al., 2016b). One of the reasons why the mismatch between experimental and computational results occurs could be related to the experimental error in the solids volume fraction measurements, which is entering the computation of the solids mass flux. Mass should be conserved throughout the axial direction of the riser at steady state. However, solids mass fluxes computed by PIV/DIA were of 32 ± 12 kg/m²s, when complete solids carryover was performed (Carlos Varas et al., 2016b).

Particles motion is strongly affected by drag force and collisional parameters. From the available drag closures, Ergun and Wen and Yu drag closure, was found to overestimate the drag force in circulating fluidised systems as other authors previously reported (Li et al., 2009). Thus, we employed the Beetstra correlation which was developed from Lattice-Boltzmann simulations (Beetstra et al.,

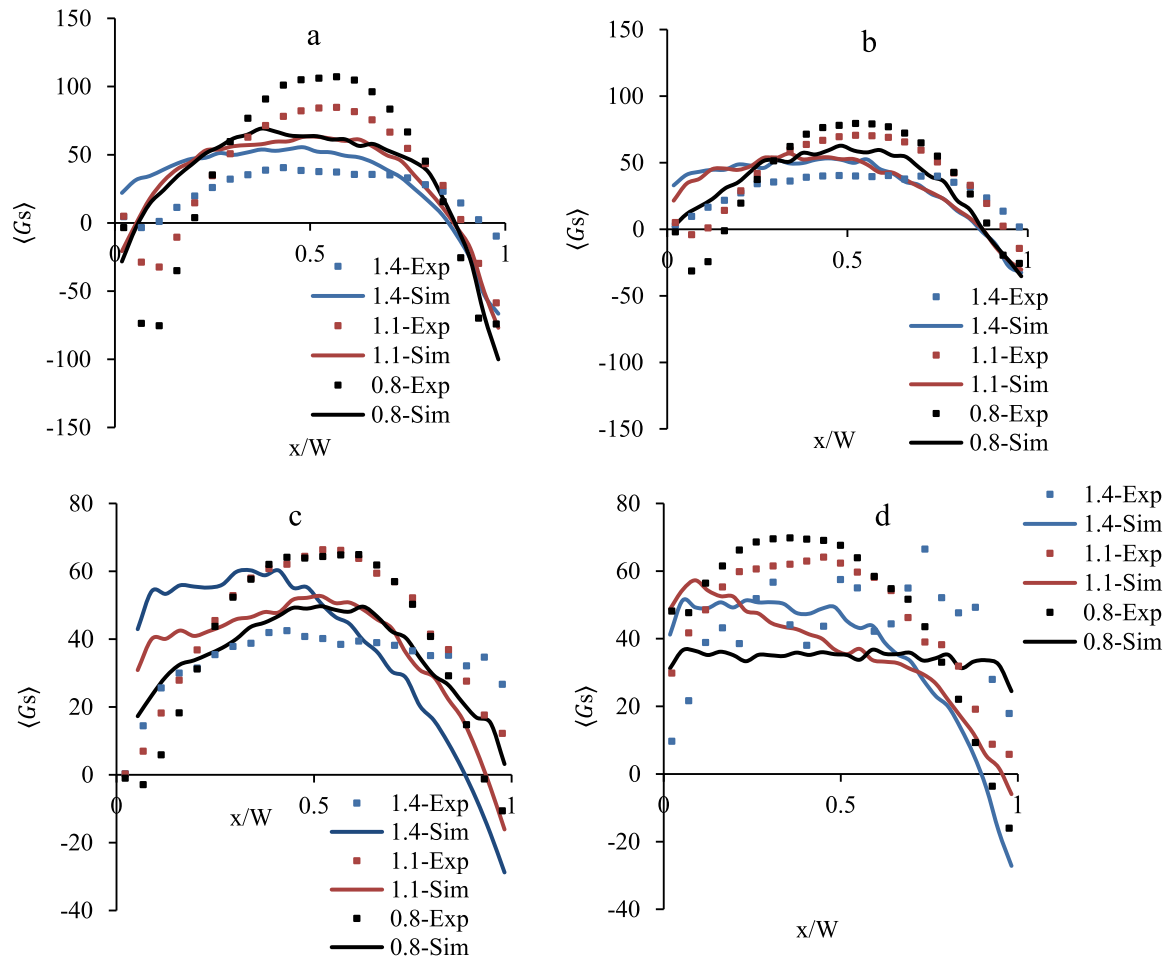


Fig. 5. Cross sectional profiles of solids mass flux. a) $U=5.55$ m/s. b) $U=5.95$ m/s. c) $U=6.35$ m/s. d) $U=6.74$ m/s.

2007). Accurate drag closures are being investigated over the last decades and DNS studies of freely evolving particle structures under high particle Re number are still under development (Tang et al., 2015; Tenneti et al., 2016).

4.3. Clusters

4.3.1. Cluster frequency

Clusters were detected along the entire length of the riser accordingly with the method described in previous sections. The centre of mass of each cluster was located in the riser domain. The centre of mass of all detected clusters was binned throughout the width of the riser reactor. In Fig. 6, the number of clusters per frame in each one of these bins is plotted. The number of clusters present corresponds well to the experimental data in terms of magnitude. However, it can be noticed from the experimental and computational results that more clusters are present close to the walls in comparison to the core of the reactor, providing another evidence of the core-annulus behaviour that prevails in the riser. This is consistent with the asymmetries observed in the solids volume fraction and solids mass flux profiles. It has to be noted that the total number of detected clusters does not correspond to the total number of clusters that are formed in an experiment or simulation, since the cluster formation is not specifically tracked. Thus, the total number of clusters are normalised by the corresponding number of images or input files.

By any means, the Euler-Lagrangian model provides a relatively accurate estimation of the cluster presence in the real experiment.

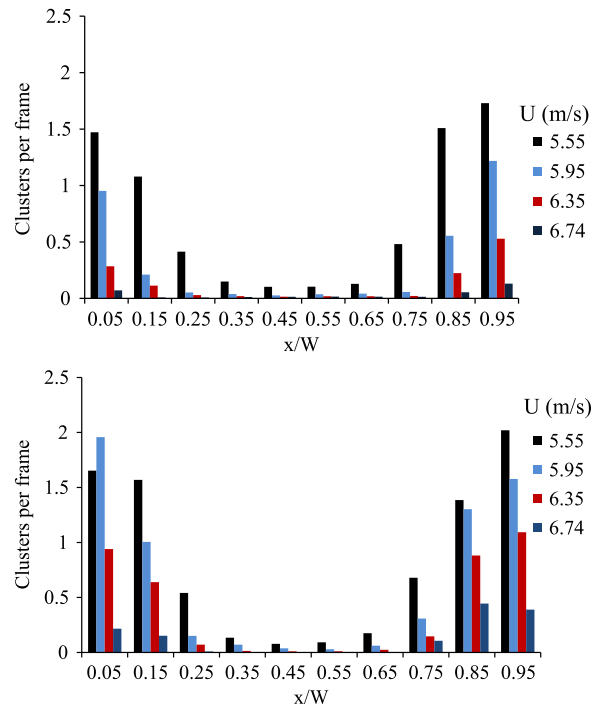


Fig. 6. Cluster frequency. Top: Experiments. Bottom: CFD-DEM simulations.

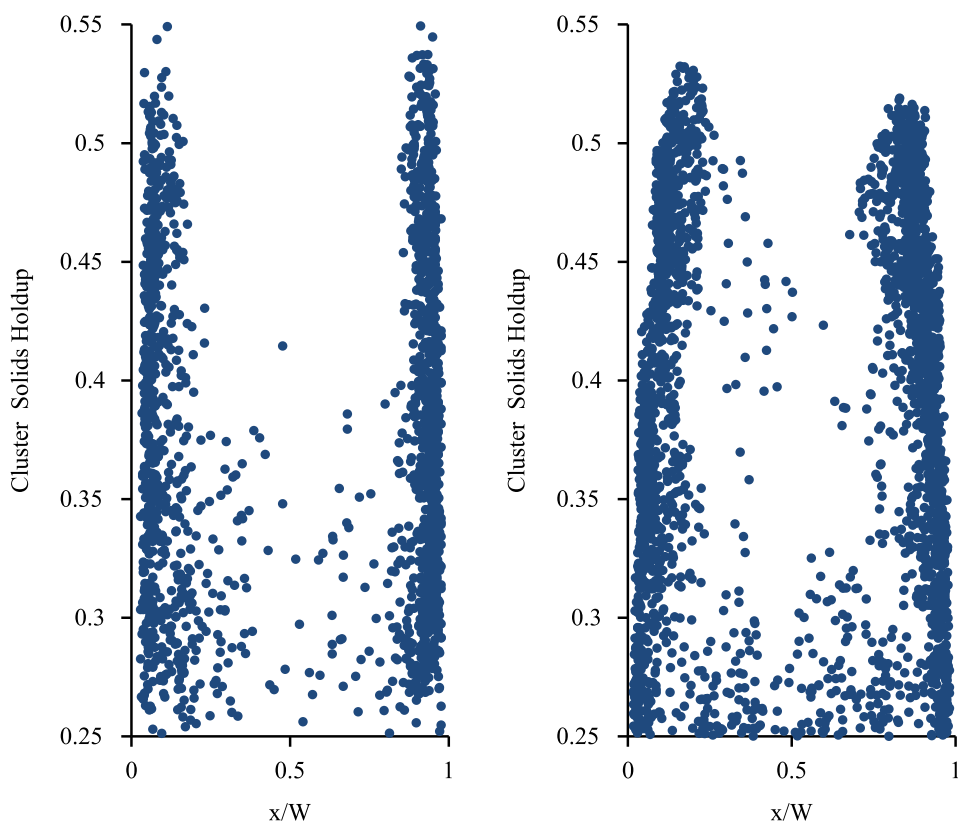


Fig. 7. Cluster solids holdup vs cluster centroid width location. Left: Experiments. Right: Simulations. $U=5.95$ m/s.

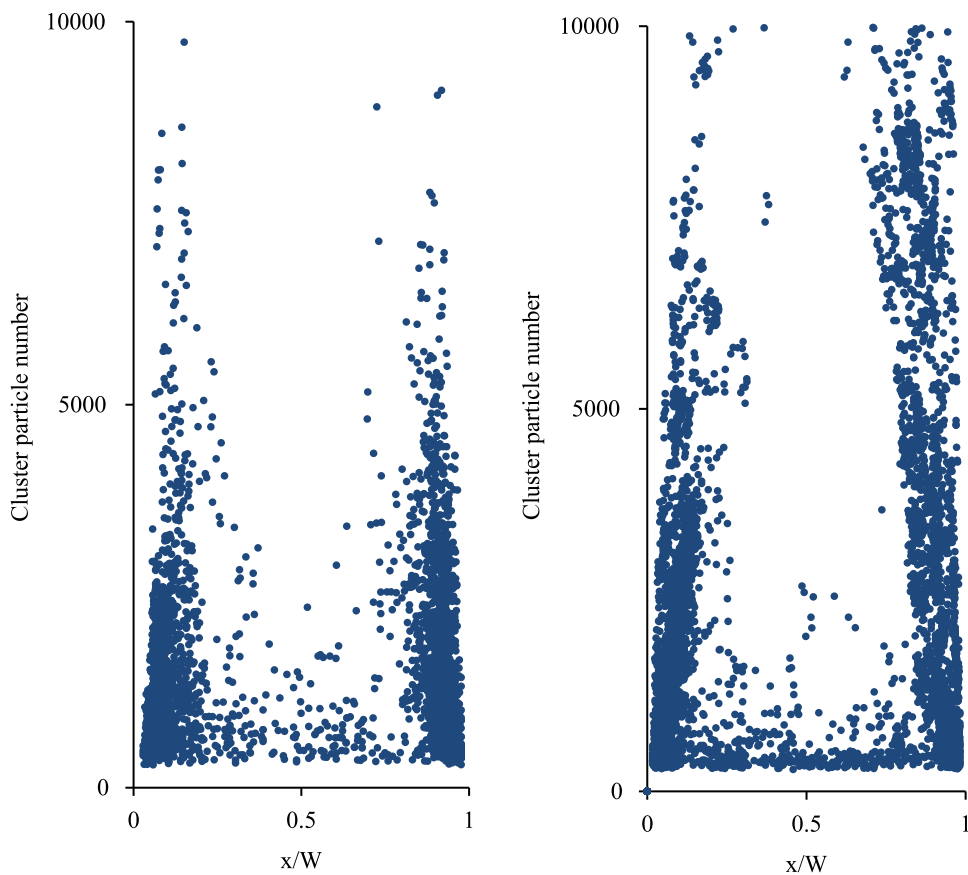


Fig. 8. Cluster mass vs cluster centroid. Left: Experiments. Right: CFD-DEM simulations. $U=5.95$ m/s.

4.3.2. Clusters size and internal solids volume fraction

The mean cluster solids holdup can be easily computed once clusters are identified. The solids volume fraction corresponding to the Cartesian cells that are occupied by a cluster are averaged to obtain this property. Thus, the averaged cluster internal solids volume fraction is $\bar{\varphi}_{\text{cluster}} = \frac{\sum \varphi_s}{N_{\text{occupied}}}$.

In Fig. 7, computational and experimental results are shown. In this case, we compare, the typical bulk cluster solids holdup of the system at $U = 5.95$ m/s. Cluster centroids are plotted along the dimensionless width of the pseudo-2D riser reactor in the abscissa, and their respective mean solids volume fraction in the ordinates.

We can observe that the densest clusters reside only close to walls. Due to the high slip velocities in the core of the system, clusters in the centre of the system are rather dilute. What can be noticed as well is that, in experiments cluster centroids are still quite close to the walls at high solids holdup values. However, in simulations, cluster centroids shift towards the centre as long as their solids density is higher, conveying that clustering could be a relatively slow process, which requires aggregation of many particles to form a dense cluster core.

Fig. 8, corroborates this observation. Clusters are heavier in simulations than in experiments, reaching almost 8 g by weight. Whereas, in experiments, the heavier ones are mostly lighter than 6 g. It could be that cluster lifetime is longer in simulations than in experiments, promoting the cluster growth.

4.3.3. Cluster area

The projected cluster area was also quantified in an attempt to further characterize the clusters that were formed in the system. The number of cells occupied by a cluster was used to estimate their corresponding projected area. Fig. 9 shows the probability distribution function of the cluster area. Due to the used cluster-definition areas are always larger than $6.0 \times 10^{-5} \text{ m}^2$ so there is a cutoff on the left side of the graph.

It is shown, that the cluster size distribution predicted by the model is close to the one from experiments. The size distribution function shows that in simulations larger clusters are formed than in experiments. This overestimation of large clusters is balanced with an underestimation of smaller clusters, as Fig. 9 illustrates.

4.3.4. Cluster aspect ratio

In Fig. 10, we compare the aspect ratio of clusters. This parameter is obtained by fitting clusters with an ellipsoidal shape by means of the Matlab 'regionprops' function. The degree of elongation of a cluster is characterised by the ratio between the major and the minor axis of these ellipses. Clusters are usually found to have elongated shapes, especially near the walls.

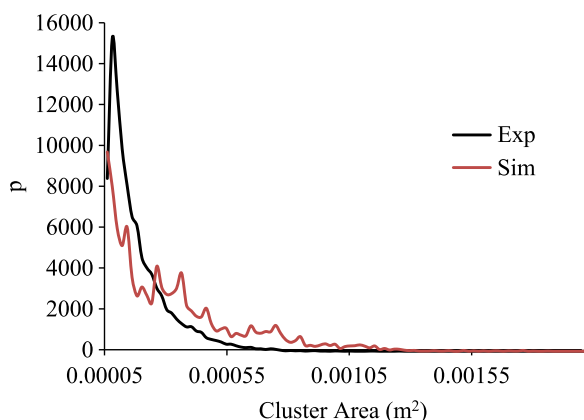


Fig. 9. Cluster area probability distribution function. $U = 5.95$ m/s.

In simulations, we observe that clusters with an aspect ratio greater than 10 are formed close to the walls, and these are especially larger near the left side wall, otherwise a quite symmetric distribution is obtained.

4.3.5. Cluster velocity

To determine the velocity of a cluster, we proceed in similar manner as described in the earlier section. Particle velocities of grids, which are occupied by each cluster are averaged and weighted by their respective solids volume fraction. In this way, we compute a particle-weighted cluster mean velocity.

In Fig. 11 (Left), we see a cluster moving downwards close to the wall. A qualitative correspondence between simulations and experiments is observed in this figure. We see that the particles inside the cluster move downwards, and others following the cluster trajectory are "sucked" into the cluster. Near the cluster core, we also see that isolated particles collide with the cluster and move inwards (towards the riser core). This phenomenon can be driven by the gas flow that tries to circumvent clusters rather than fully penetrating into the cluster phase. In the snapshot, we see that CFD-DEM captures well these phenomena.

In Fig. 12, we show cluster velocities from experiments and simulations at the same operating conditions. We notice that in experiments and simulations, cluster centroids describe a core annulus flow. In experiments, clusters close to the walls are those which have a higher probability to fall downwards reaching velocities up to -2 m/s, whereas, in the riser core, dilute clusters travel upwards with velocities up to 1.84 m/s.

The data clouds of the cluster mean velocities are comparable to those in experiments. In simulations, it can also be noticed that centroids of clusters falling downwards shift towards the centre of the domain, possibly due to their larger size. Clusters formed in the Euler-Lagrangian simulation have lower velocity magnitudes. The cluster centroids also describe a core annulus-shape although clusters in the riser core could reach lower velocities than in experiments.

4.3.6. Granular temperature

It has been shown that CFD-DEM is an accurate model to predict complex clustering phenomena. Thus, we further characterize clusters by relating their centroid location to their corresponding granular temperature. Several researchers quantified granular temperature in order to evaluate the velocity fluctuations of particles in riser systems (Shuyan et al., 2005; Neri and Gidaspow, 2000; Mathiesen et al., 2000; Breault et al., 2005; Kashyap et al., 2011).

It is expected that velocity fluctuations are higher in dilute regions in comparison to densely packed clusters, where particles tend to follow the same trajectory (Breault et al., 2005).

For each computational cell, the granular temperature θ_{cluster} was computed as follows:

$$\theta = \frac{1}{3} \left(\left(\frac{\sum_{p=1}^n (v_{p,x} - \bar{v}_{p,x})^2 m_p}{m_{p,\text{cell}}} \right) + \left(\frac{\sum_{p=1}^n (v_{p,y} - \bar{v}_{p,y})^2 m_p}{m_{p,\text{cell}}} \right) + \left(\frac{\sum_{p=1}^n (v_{p,z} - \bar{v}_{p,z})^2 m_p}{m_{p,\text{cell}}} \right) \right) \quad (6)$$

where $m_{p,\text{cell}}$ is the total mass of all particles present in the cell, \bar{v}_p is the cell-averaged particle velocity, v_p is the particle velocity, and n is the total number of particles in the cell.

These data were computed every 5 ms of simulation time and post-processed to relate these data to the solids concentration of the system. Thus, instantaneous solids volume fraction data were

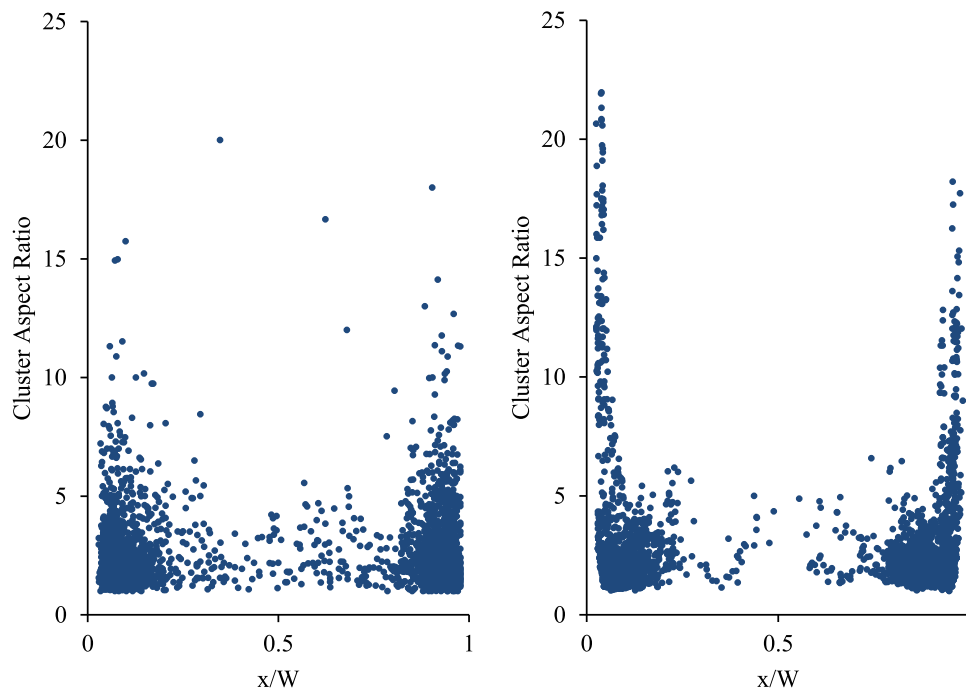


Fig. 10. Cluster aspect ratio. Left: PIV/DIA experiments. Right: CFD-DEM simulations. $U=5.95$ m/s.

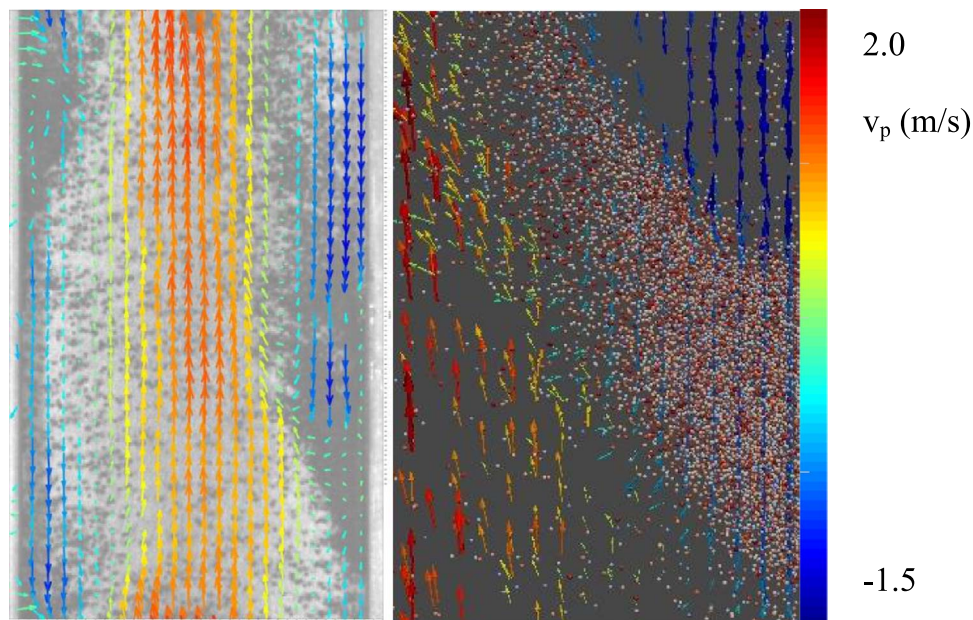


Fig. 11. Snapshots of cluster motion. Left: Particle velocity field from PIV-DIA experiments. Right: Zoomed snapshot of a particle cluster from CFD-DEM with the particle velocity field superimposed at Eulerian coordinates.

binned into 67 classes ranging from $\phi_s=0.01$ to $\phi_s=0.67$. Corresponding values of granular temperature were particle-averaged for each one of these bins. The results of this post-processing are shown in Fig. 13.

In Fig. 13, it is seen that the granular temperature reaches a maximum and then decays in denser regions. Qualitatively, this is in good agreement with findings reported by previous authors (Gidaspow and Huilin, 1998; Shuyan et al., 2005).

In Fig. 14, we show the granular temperature of around 4000 clusters with their respective centroid width location. It is expected that clusters in the core have higher mobility due to a more intense interaction with the gas phase. However the data cloud near the walls do not provide a clear visualisation of this pattern.

Thus, the average granular temperature of core clusters ($0.23 < x/W < 0.77$) and wall-clusters ($x/W < 0.23$ and $x/W > 0.77$) was computed. These amount to 58 and $46 \text{ cm}^2/\text{s}^2$ respectively.

5. Conclusions

In this work, we have shown that Eulerian-Lagrangian models are a suitable framework to predict mesoscale particle structures under riser flow conditions. A thorough validation of the model with full-field experimental data has been performed under dilute fast fluidisation conditions. Solids volume fraction and axial solids fluxes computational data are in close agreement with experiments.

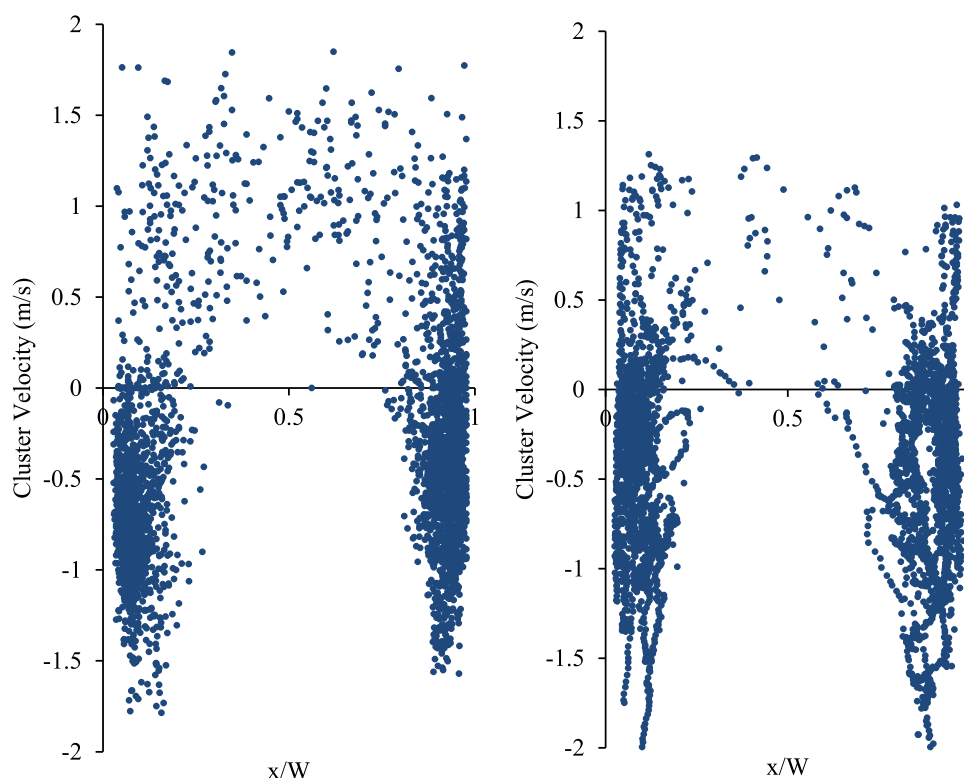


Fig. 12. Mean cluster axial velocity vs centroid location over 1000 experimental images/output CFD-DEM files (around 4000 clusters). Left: PIV/DIA experiments. Right: CFD-DEM simulations. $U=5.95$ m/s.

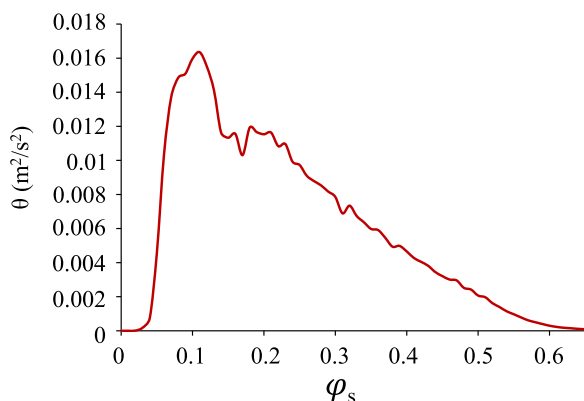


Fig. 13. Average granular temperature vs solids volume fraction. CFD-DEM data.

We conclude that for this case of riser flow CFD-DEM simulations are capable of predicting particle heterogeneities well when computational cell sizes of 3 particle diameters are used. This is in agreement with earlier findings for bubbling fluidisation (e.g. Bokkers, 2005; Wang et al., 2009b; Wang et al., 2010).

In addition, we have shown that the cluster distribution predicts well the core-annulus behaviour of riser systems as well as it shows good agreement with experimental data. However, solids mass flux profiles show some degree of mismatch with experimental data. The reason of this could originate from the error propagation of solids volume fraction experimental measurements into the solids mass flux computation (Carlos Varas et al., 2016b).

Clusters were characterised by their size, velocity, aspect ratio and size. The distributions of all these properties were in close correspondence with experimental results. Thus it has been shown that CFD-DEM can predict accurately key features of heterogeneous riser flow, including cluster properties that have a key influence on the quality of the gas-solid contact such as internal

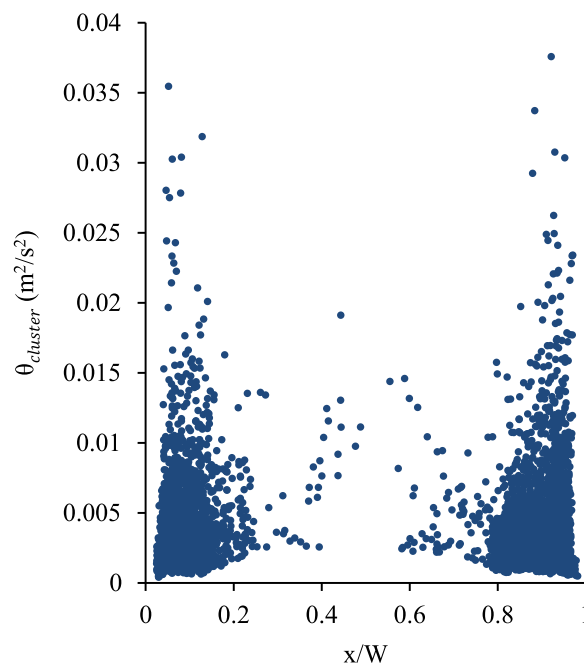


Fig. 14. Cluster granular temperature vs cluster centroid location. CFD-DEM data.

solids holdup, aspect ratio and velocity. However, some CFD-DEM simulations over predict the amount of larger clusters inside the system. Thus, more insight about the influence of drag force and collision parameters on the cluster characteristics could be relevant to predict cluster phenomena even more accurately.

These data sets cover only dilute riser conditions with Geldart D particles. Thus, more full-field experimental references are needed to have a better overview of the reliability of Euler-Lagrangian models under different fluidisation regimes and Archimedes numbers. This

investigation highlights the possibility to simulate accurately CFB riser systems by means of CFD-DEM, without making unrealistic assumptions regarding cluster properties that are needed in more coarse grained simulation methods. Clearly, if CFD-DEM simulations are to be applied to bigger systems than our 'simple' pseudo-2D lab-scale riser efficient massively parallel CFD-DEM codes need to be used. These, however, are currently being developed by several groups (Berger et al., 2015; Amritkar et al., 2014; Xu et al., 2012).

Acknowledgement

This paper is an extension of a conference paper that was presented at the Eleventh International Conference on CFD in the Minerals and Process Industries (CFD2015), and was nominated for submission to Chemical Engineering Science based on its designation as a high-quality paper of relevance to chemical engineering.

This research is funded by the Netherlands Organisation for Scientific Research (NWO) under project number 713.012.002.

References

- Agrawal, K., Loezos, P.N., Syamlal, M., Sundaresan, S., 2001. The role of meso-scale structures in rapid gas-solid flows. *J. Fluid Mech.* 445, 151–185. <http://dx.doi.org/10.1017/S0022112001005663>.
- Amritkar, A., Deb, S., Tafti, D., 2014. Efficient parallel CFD-DEM simulations using OpenMP. *J. Comput. Phys.* 256, 501–519. <http://dx.doi.org/10.1016/j.jcp.2013.09.007>.
- Beetstra, R., Van der Hoef, M.A., Kuipers, J.A.M., 2007. Numerical study of segregation using a new drag force correlation for polydisperse systems derived from lattice-Boltzmann simulations. *Chem. Eng. Sci.* 62, 246–255.
- Berger, R., Kloss, C., Kohlmeyer, A., Pirker, S., 2015. Hybrid parallelization of the LIGGGHTS open-source DEM code. *Powder Technol.* 278, 234–247. <http://dx.doi.org/10.1016/j.powtec.2015.03.019>.
- Bokkers, G.A., 2005. Multi-level Modelling Of The Hydrodynamics In Gas Phase Polymerization Reactors (Ph.D. Thesis). University of Twente, Enschede, Netherlands.
- Breault, R.W., Ludlow, C.J., Yue, P.C., 2005. Cluster particle number and granular temperature for cork particles at the wall in the riser of a CFB. *Powder Technol.* 149 (2–3), 68–77. <http://dx.doi.org/10.1016/j.powtec.2004.11.003>.
- Brereton, C.M.H., Grace, J.R., 1993. Microstructural aspects of the behaviour of circulating fluidized beds. *Chem. Eng. Sci.* 48, 2565–2572. [http://dx.doi.org/10.1016/0009-2509\(93\)80267-T](http://dx.doi.org/10.1016/0009-2509(93)80267-T).
- Cabezas-Gómez, L., Da Silva, R.C., Navarro, H.A., Milioli, F.E., 2008. Cluster identification and characterization in the riser of a circulating fluidized bed from numerical simulation results. *Appl. Math. Model.* 32 (3), 327–340. <http://dx.doi.org/10.1016/j.apm.2006.12.005>.
- Capecelatro, J., Peipat, P., Desjardins, O., 2014. Numerical characterization and modeling of particle clustering in wall-bounded vertical risers. *Chem. Eng. J.* 245, 295–310. <http://dx.doi.org/10.1016/j.cej.2014.02.040>.
- Carlos Varas, A.E., Peters, E.A.J.K., Deen, N.G., Kuipers, J.A.M., 2016a. Solids volume fraction measurements on riser flow using a temporal-histogram based DIA method. *AIChE J.* 62 (8), 2681–2698. <http://dx.doi.org/10.1002/aic.15243s>.
- Carlos Varas, A.E., Peters, E.A.J.K., Kuipers, J.A.M., 2016b. Experimental study of full field riser hydrodynamics by PIV/DIA coupling Fluidization XV. Full manuscript submitted to Powder Technology.
- Cheng, C., Li, F., Qi, H., 2012. Modeling of the flue gas desulfurization in a CFB riser using the Eulerian approach with heterogeneous drag coefficient. *Chem. Eng. Sci.* 69 (1), 659–668. <http://dx.doi.org/10.1016/j.ces.2011.11.035>.
- Chew, J.W., Hays, R., Findlay, J.G., Knowlton, T.M., Reddy Karri, S.B., Cocco, R.A., Hrenya, C.M., 2012. Cluster characteristics of Geldart Group B particles in a pilot-scale CFB Riser. I. Monodisperse systems. *Chem. Eng. Sci.* 68 (1), 72–81. <http://dx.doi.org/10.1016/j.ces.2011.09.012>.
- Cundall, P.A., Strack, O.D.L., 1979. A discrete numerical model for granular assemblies. *Géotechnique* 29 (1), 47–65.
- Deen, N.G., Van Sint Annaland, M., Van der Hoef, M.A., Kuipers, J.A.M., 2007. Review of discrete particle modeling of fluidized beds. *Chem. Eng. Sci.* 62 (1–2), 28–44. <http://dx.doi.org/10.1016/j.ces.2006.08.014>.
- Gidaspow, D., Huilin, L., 1998. Equation of state and radial distribution functions of FCC particles in a CFB. *AIChE J.* 44 (2), 279–293. <http://dx.doi.org/10.1002/aic.690440207>.
- Goldschmidt, M.J.V., Beetstra, R., Kuipers, J.A.M., 2004. Hydrodynamic modelling of dense gas-fluidised beds: comparison and validation of 3D discrete particle and continuum models. *Powder Technol.* 142 (1), 23–47. <http://dx.doi.org/10.1016/j.powtec.2004.02.020>.
- Guenther, C., Breault, R., 2007. Wavelet analysis to characterize cluster dynamics in a circulating fluidized bed. *Powder Technol.* 173 (3), 163–173. <http://dx.doi.org/10.1016/j.powtec.2006.12.016>.
- Harris, A.T., Davidson, J.F., Thorpe, R.B., 2002. The prediction of particle cluster properties in the near wall region of a vertical riser. *Powder Technol.* 127, 128–143. [http://dx.doi.org/10.1016/S0032-5910\(02\)00114-6](http://dx.doi.org/10.1016/S0032-5910(02)00114-6).
- Hartge, E.U., Ratschow, L., Wischniewski, R., Werther, J., 2009. CFD-simulation of a circulating fluidized bed riser. *Particuology* 7 (4), 283–296. <http://dx.doi.org/10.1016/j.partic.2009.04.005>.
- Helland, E., Bournot, H., Occelli, R., Tadriss, L., 2007. Drag reduction and cluster formation in a circulating fluidised bed. *Chem. Eng. Sci.* 62 (1–2), 148–158. <http://dx.doi.org/10.1016/j.ces.2006.08.012>.
- Hoomans, B.P.B., Kuipers, J.A.M., Van Swaaij, W.P.M., 2000. Granular dynamics simulation of segregation phenomena in bubbling gas-fluidised beds. *Powder Technol.* 109, 41–48. [http://dx.doi.org/10.1016/S0032-5910\(99\)00225-9](http://dx.doi.org/10.1016/S0032-5910(99)00225-9).
- Hoomans, B.P.B., Kuipers, J.A.M., Briels, W.J., Van Swaaij, W.P.M., 1996. Discrete particle simulation of bubble and slug formation in a two-dimensional gas-fluidised bed: a hard-sphere approach. *Chem. Eng. Sci.* 51 (1), 99–118. [http://dx.doi.org/10.1016/0009-2509\(95\)00271-5](http://dx.doi.org/10.1016/0009-2509(95)00271-5).
- Horio, M., Kuroki, H., 1994. Three-dimensional flow visualization of dilutely dispersed solids in bubbling and circulating fluidized beds. *Chem. Eng. Sci.* 49 (15), 2413–2421. [http://dx.doi.org/10.1016/0009-2509\(94\)E0071-W](http://dx.doi.org/10.1016/0009-2509(94)E0071-W).
- Jajcevic, D., Siegmund, E., Radeke, C., Khinast, J.G., 2013. Large-scale CFD-DEM simulations of fluidized granular systems. *Chem. Eng. Sci.* 98, 298–310. <http://dx.doi.org/10.1016/j.ces.2013.05.014>.
- Johnsson, H., Johnsson, F., 2001. Measurements of local solids volume-fraction in fluidized bed boilers. *Powder Technol.* 115, 13–26. [http://dx.doi.org/10.1016/S0032-5910\(00\)00270-9](http://dx.doi.org/10.1016/S0032-5910(00)00270-9).
- Kashyap, M., Chalermisinsuwan, B., Gidaspow, D., 2011. Measuring turbulence in a circulating fluidized bed using PIV techniques. *Particuology* 9, 572–588. <http://dx.doi.org/10.1016/j.partic.2011.06.007>.
- Li, J., Kuipers, J.A.M., 2003. Gas-particle interactions in dense gas-fluidized beds. *Chem. Eng. Sci.* 58 (3–6), 711–718. [http://dx.doi.org/10.1016/S0009-2509\(02\)00599-7](http://dx.doi.org/10.1016/S0009-2509(02)00599-7).
- Li, J., Kuipers, J.A.M., 2007. Effect of competition between particle-particle and gas-particle interactions on flow patterns in dense gas-fluidized beds. *Chem. Eng. Sci.* 62 (13), 3429–3442. <http://dx.doi.org/10.1016/j.ces.2007.01.086>.
- Li, J., Kwauk, M., 1994. Particle-Fluid Two-Phase Flow EMMS. Metallurgical Industry Press, Beijing.
- Li, P., Lan, X., Xu, C., Wang, G., Lu, C., Gao, J., 2009. Drag models for simulating gas-solid flow in the turbulent fluidization of FCC particles. *Particuology* 7, 269–277. <http://dx.doi.org/10.1016/j.partic.2009.03.010>.
- Lu, H., Wang, S., Yurong, H., Ding, J., Liu, G., Hao, Z., 2008. Numerical simulation of flow behavior of particles and clusters in riser using two granular temperatures. *Powder Technol.* 182 (2), 282–293. <http://dx.doi.org/10.1016/j.powtec.2007.09.003>.
- Lu, L., Xu, J., Ge, W., Yue, Y., Liu, X., Li, J., 2014. EMMS-based discrete particle method (EMMS-DPM) for simulation of gas-solid flows. *Chem. Eng. Sci.* 120, 67–87. <http://dx.doi.org/10.1016/j.ces.2014.08.004>.
- Lun, C.K.K., Savage, S.B., Jeffrey, D.J., Chepurini, N., 1984. Kinetic theories for granular flow: inelastic particles in Couette flow and slightly inelastic particles in a general flow field. *J. Fluid Mech.* 140, 223. <http://dx.doi.org/10.1017/S0022112084000586>.
- Manyele, S.V., Parssinen, J.H., Zhu, J.-X., 2002. Characterizing particle aggregates in a high-density and high flux CFB riser. *Chem. Eng. J.* 88, 151–161.
- Mathiesen, V., Solberg, T., Hjertager, B.H., 2000. An experimental and computational study of multiphase flow behavior in a circulating fluidized bed. *Int. J. Multiph. Flow* 26, 387–419. [http://dx.doi.org/10.1016/S0301-9322\(99\)00027-0](http://dx.doi.org/10.1016/S0301-9322(99)00027-0).
- Naren, P.R., Lali, A.M., Ranade, V.V., 2007. Evaluating EMMS model for simulating high solid flux risers. *Chem. Eng. Res. Des.* 85, 1188–1202. <http://dx.doi.org/10.1205/cherd.06077>.
- Neri, A., Gidaspow, D., 2000. Riser hydrodynamics: simulation using kinetic theory. *AIChE J.* 46 (1), 52–67. <http://dx.doi.org/10.1002/aic.690460108>.
- Ouyang, J., Li, J., 1999. Discrete simulations of heterogeneous structure and dynamic behavior in gas-solid fluidization. *Chem. Eng. Sci.* 54 (22), 5427–5440. [http://dx.doi.org/10.1016/S0009-2509\(99\)00275-4](http://dx.doi.org/10.1016/S0009-2509(99)00275-4).
- Panday, R., Shadle, L.J., Shahnam, M., Cocco, R., Issangya, A., Spenik, J.S., Ludlow, J.C., et al., 2014. Challenge problem: 1. Model validation of circulating fluidized beds. *Powder Technol.* 258, 370–391. <http://dx.doi.org/10.1016/j.powtec.2014.02.010>.
- Sharma, A.K., Tuzla, K., Matsen, J., Chen, J.C., 2000. Parametric effects of particle size and gas velocity on cluster characteristics in fast fluidized beds. *Powder Technol.* 111, 114–122. [http://dx.doi.org/10.1016/S0032-5910\(00\)00247-3](http://dx.doi.org/10.1016/S0032-5910(00)00247-3).
- Shuai, W., Guodong, L., Huilin, L., Pengfei, X., Yunchao, Y., Gidaspow, D., 2012. A cluster structure-dependent drag coefficient model applied to risers. *Powder Technol.* 225, 176–189. <http://dx.doi.org/10.1016/j.powtec.2012.04.006>.
- Shuyan, W., Huanpeng, L., Huilin, L., Wentie, L., Ding, J., Wei, L., 2005. Flow behavior of clusters in a riser simulated by direct simulation Monte Carlo method. *Chem. Eng. J.* 106 (3), 197–211. <http://dx.doi.org/10.1016/j.cej.2004.12.036>.
- Shuyan, W., Xiang, L., Huilin, L., Long, Y., Dan, S., Yurong, H., Yonglong, D., 2009. Numerical simulations of flow behavior of gas and particles in spouted beds using frictional-kinetic stresses model. *Powder Technol.* 196 (2), 184–193. <http://dx.doi.org/10.1016/j.powtec.2009.07.020>.
- Soong, C.H., Tuzla, K., Chen, J.C., 1993. Identification of particle clusters in circulating fluidized bed. *Circulating Fluidized Bed Technology IV*.
- Sundaresan, S., 2013. Role of hydrodynamics on chemical reactor performance. *Curr. Opin. Chem. Eng.* 2 (3), 325–330. <http://dx.doi.org/10.1016/j.coche.2013.06.003>.

- Tang, Y., Peters, E.A.J.F., Kuipers, J.A.M., Kriebitzsch, S.H.L., Hoef, van der, M.A., 2015. A new drag correlation from fully resolved simulations of flow past mono-disperse static arrays of spheres. *AIChE J.* 61 (2), 688–698.
- Tenneti, S., Mehrabadi, M., Subramaniam, S., 2016. Stochastic Lagrangian model for hydrodynamic acceleration of inertial particles in gas-solid suspensions. *J. Fluid Mech.* 788, 695–729.
- Tsuji, Y., Kawaguchi, T., Tanaka, T., 1993. Discrete particle simulation of two-dimensional fluidized bed. *Powder Technol.* 77, 79–87. [http://dx.doi.org/10.1016/0032-5910\(93\)85010-7](http://dx.doi.org/10.1016/0032-5910(93)85010-7).
- Tsuji, Y., Tanaka, T., Yonemura, S., 1998. Cluster patterns in circulating fluidized beds predicted by numerical simulation (discrete particle model versus two-fluid model). *Powder Technol.* 95 (3), 254–264. [http://dx.doi.org/10.1016/S0032-5910\(97\)03349-4](http://dx.doi.org/10.1016/S0032-5910(97)03349-4).
- Tsuo, Y.P., Gidaspow, D., 1990. Computation of flow patterns in circulating fluidized beds. *AIChE J.* 36 (6), 885–896. <http://dx.doi.org/10.1002/aic.690360610>.
- Tsuzuki, S., Aoki, T., 2016. Large-scale particle simulations for Debris flows using dynamic load balance on a GPU-rich supercomputer. *Geophys. Res. Abstr.* 18, 4857.
- Vreman, B., Geurts, B.J., Deen, N.G., Kuipers, J.A.M., Kuerten, J.G.M., 2009. Two- and four-way coupled Euler-Lagrangian large-eddy simulation of turbulent particle-laden channel flow. *Flow., Turbul. Combust.* 82 (1), 47–71. <http://dx.doi.org/10.1007/s10494-008-9173-z>.
- Walther, J.H., Sbalzarini, I.F., 2009. Large-scale parallel discrete element simulations of granular flow. *Eng. Comput.* 26 (6), 688–697.
- Wang, J., Ge, W., Li, J., 2008. Eulerian simulation of heterogeneous gas–solid flows in CFB risers: EMMS-based sub-grid scale model with a revised cluster description. *Chem. Eng. Sci.* 63, 1553–1571. <http://dx.doi.org/10.1016/j.ces.2007.11.023>.
- Wang, S., Li, X., Lu, H., Yu, L., Ding, J., Yang, Z., 2009a. DSMC prediction of granular temperatures of clusters and dispersed particles in a riser. *Powder Technol.* 192 (2), 225–233. <http://dx.doi.org/10.1016/j.powtec.2009.01.008>.
- Wang, J., Van der Hoef, M.A., Kuipers, J.A.M., 2009b. Why the two-fluid model fails to predict the bed expansion characteristics of Geldart A particles in gas-fluidized beds: a tentative answer. *Chem. Eng. Sci.* 64, 622–625.
- Wang, J., Van der Hoef, M.A., Kuipers, J.A.M., 2010. CFD study of the minimum bubbling velocity of Geldart A particles in gas-fluidized beds. *Chem. Eng. Sci.* 65, 3772–3785. <http://dx.doi.org/10.1016/j.ces.2010.03.023>.
- Xu, M., Chen, F., Liu, X., Li, J., 2012. Discrete particle simulation of gas-solid two-phase flows with multiscale CPU-GPU hybrid computation. *Chem. Eng. J.* 207–208, 746–757. <http://dx.doi.org/10.1016/j.ces.2012.07.049>.
- Yang, J., Zhu, J., 2015. Cluster identification using image processing. *Particuology* 23, 16–24. <http://dx.doi.org/10.1016/j.partic.2014.12.004>.
- Yang, S., Luo, K., Zhang, K., Qiu, K., Fan, J., 2015. Numerical study of a lab-scale double slot-rectangular spouted bed with the parallel CFD-DEM coupling approach. *Powder Technol.* 272, 85–99. <http://dx.doi.org/10.1016/j.powtec.2014.11.035>.
- Yerushalmi, J., Cankurt, N.T., 1979. Further studies of the regimes of fluidization. *Powder Technol.* 24, 187–205. [http://dx.doi.org/10.1016/0032-5910\(79\)87036-9](http://dx.doi.org/10.1016/0032-5910(79)87036-9).